



ORIGINAL ARTICLE

Mechanistic and kinetic aspects of Natamycin interaction with serum albumin using spectroscopic and molecular docking methods



Maryam Azimirad^a, Fatemeh Javaheri-Ghezeldizaj^b, Reza Yekta^c, Jafar Ezzati Nazhad Dolatabadi^{d,*}, Mohammadali Torbati^{a,*}

^a Department of Food Science and Technology, Faculty of Nutrition and Food Sciences, Nutrition Research Center, Tabriz University of Medical Sciences, Tabriz, Iran

^b Department of Food Science and Technology, National Nutrition and Food Technology Research Institute, Faculty of Nutrition Sciences, Food Science and Technology, Shahid Beheshti University of Medical Sciences, Tehran, Iran

^c Pharmaceutical Analysis Research Center, Tabriz University of Medical Sciences, Tabriz, Iran

^d Drug Applied Research Center, Tabriz University of Medical Sciences, Tabriz, Iran

Received 21 February 2023; accepted 30 May 2023

Available online 5 June 2023

KEYWORDS

Natamycin;
Serum albumin;
Spectroscopic technique;
Surface plasmon resonance;
Docking simulation

Abstract Natamycin (NT) is a polyene natural antimycotic, which has an antimicrobial effect against yeasts and molds and is used as a preservative in the food industry. In the present study, we evaluated NT interaction with bovine serum albumin (BSA) through surface plasmon resonance (SPR) and several spectroscopic techniques, which are accompanied by a molecular docking study. According to the results, the intensity of BSA fluorescence decreased by adding different concentrations of NT. The fluorescence quenching results showed that NT reduces the intensity of BSA fluorescence by forming a complex with BSA through a hybrid quenching. Binding constant decreases from 18.73 to 2.13 (10^2 M^{-1}) with increasing temperature, which indicates a decrease in complex formation owing to the interaction of NT with BSA. Negative values of ΔH° and ΔS° confirmed that van der Waals forces and hydrogen bonds are the basic forces in the interaction of NT with BSA. Moreover, increasing the equilibrium constants values with increasing temperature indicated that BSA binding to NT decreased. Finally, BSA interaction occurring with NT through Ser 109, Asp 111, Lys 114, Leu 115, Glu 424, and Arg 458 have been verified via molecular docking analysis.

* Corresponding authors.

E-mail addresses: ezzatij@tbzmed.ac.ir (J. Ezzati Nazhad Dolatabadi), torbatim@tbzmed.ac.ir (M. Torbati).

Peer review under responsibility of King Saud University.



Attained results via SPR and fluorimetry showed that the binding constant between BSA and NT decreased when the temperature was raised.

© 2023 The Authors. Published by Elsevier B.V. on behalf of King Saud University. This is an open access article under the CC BY-NC-ND license (<http://creativecommons.org/licenses/by-nc-nd/4.0/>).

1. Introduction

Food additives are synthetic or natural substances that are added to food in small amounts to prolong the shelf life of the product and increase or change its attributes, including its structure, flavor, or appearance without reducing their nutritional value (Silva and Lidon, 2016). According to the EU rules, preservatives are food additives that protect food against microorganisms (fungi and/or bacteria) (Shim et al., 2011; Silva and Lidon, 2016). Moreover, the side effects of food additives on public health have become an argued subject in recent years (Javaheri-Ghezeldizaj et al., 2020). Natamycin (NT) (pimaricin, pimarinin) is a polyene natural antimycotic that is produced in immersed culture by different strains of actinomycetes, like Streptomyces, Chattanooga, Streptomyces, gilvosporeus, and Streptomyces. natalensis (Pintado et al., 2010; Elsayed et al., 2013). NT has been used in the food industry to preserve cheese, sausages (the surface treatment), yogurt, and in some countries juices, and wine (Dalhoff and Levy, 2015). The acceptable daily intake (ADI) for NT is defined by JECFA as 0.03 mg/kg BW/day (Martínez et al., 2013). Due to its low toxicity, NT is classified by the FDA as a safe additive and in the EU as a natural preservative (da Silva et al., 2012). NT is additionally prescribed for the topical therapy of fungal infections of the eyes, throat, skin, and vaginal in humans (Levy, 2007). Since NT is a white to creamy powder, crystalline, odorless, and colorless, it causes no taste aversion in the consumer (Brik, 1981; Stark, 1999). This antifungal substance contains a large 22-carbon lactone ring that is attached to an amino sugar, a mycosamine moiety, by a glycosidic bond. NT is a polyene macrolide antibiotic and owing to its four conjugated double bonds assessed specifically as a tetraene antibiotic. NT has a low aqueous solubility (20–50 mg/L in water) and it must be used at high concentrations (Zunszain et al., 2008; Additives and Food, 2009). Most of the food available in the market contains diverse types of preservatives. These chemicals can cause immediate adverse effects including headaches, changes in energy levels, and changes in mental focus, behavior, or immune response. Or it may cause long-term effects, including an increased risk of cancer, cardiovascular disease, and other degenerative conditions. Thus, even very few doses of these additives, when consumed continuously, can lead to an irreversible toxic effect that ultimately leads to cancer and chromosomal and embryonic damage. So in recent years, researchers have paid much attention to the interaction between chemicals, especially food additives, and various biological molecules in the body (Li et al., 2007; Inetianbor et al., 2015).

Serum albumin (SA) is the most plenty biological molecule in the circulatory system of many living organisms. It is responsible for several physiological functions such as the transfer of exogenous and endogenous compounds (greasy acids, drugs, steroids, metal particles, and metabolites) (Mohammadzadeh-Aghdash et al., 2017; Szkudlarek et al., 2019). SA can increment the solubility of hydrophobic compounds and therefore, has a critical role in the absorption, metabolism, and distribution of chemicals from cells. The interaction of these chemicals with SA changes its primary and secondary structure as well as its physiological functions. So, in recent years, researchers have paid much attention to the interaction between chemicals, especially food additives, and various biological molecules in the body. Human serum albumin (HSA) consists of 585 amino acid residues in the monomer via 17 disulfide bridges that help maintain the heart-like shape. It is the foremost abundant bearer protein within the blood plasma. HSA binds to various drugs through several hydrophobic binding sites in its structure (Koch-Weser and Sellers, 1976; Petitpas et al., 2001). Another major soluble protein is bovine serum

albumin (BSA) which has 80% structural similarity to HSA (583 amino acids similar to HSA). The difference is in the number of tryptophans, in that BSA has two tryptophan amino acids, while HSA has only one tryptophan. Because of its low cost, therapeutic care, accessibility, and binding characteristics, BSA is commonly chosen as a pattern for investigating drug-protein interactions (Xu et al., 2013; Rajendiran and Thulasidhasan, 2016; Szkudlarek et al., 2019). In 2022, Khashkhashi Moghadam et al. studied the interaction behavior of cyanidin with the albumin-holo transferrin complex of human serum with a new perspective, and the results showed a moderate binding affinity between cyanidin and both proteins throughout binary and ternary systems (Khashkhashi-Moghadam et al., 2022). (Basu and Suresh Kumar, 2015) stated that the tartrazine food additive can change the chemical structure of BSA and disrupt its physiological functions (Basu and Suresh Kumar, 2015). In 2023, Zaheri et al. investigated the kinetic and thermodynamic aspects of serum albumin interaction with sodium hydrosulfite and found that sodium hydrosulfite, by forming a complex with BSA, reduces the fluorescence intensity of BSA and changes the structure of BSA (Zaheri et al., 2023). Shahabadi et al. showed that the structure of BSA changes significantly after interacting with the TBHQ (Shahabadi et al., 2011). In 2017, Asaran Darban et al. investigated the interaction between two different angiotensins I converting enzyme inhibitory peptides from gluten hydrolysate and human serum albumin and concluded that both peptides quench the fluorescence intensity of HSA through a static mechanism (Assaran Darban et al., 2017).

Given the high importance of NT consumption in the food industry, investigating its effect on the structure and function of body macromolecules such as SA can be very valuable in nutrition, food science, food chemistry, and food safety. Therefore, to understand the type of structural changes of SA and the mechanisms of SA-NT complex formation, we decided to investigate the interaction of NT with BSA using surface plasmon resonance (SPR), fluorescence and UV-Vis spectroscopies, and molecular docking analysis.

2. Material and methods

2.1. Material

N-ethyl-N-(3-dimethyl aminopropyl) carbodiimide (EDC), N-hydroxysuccinimide (NHS), phosphate-buffered saline (PBS) solution, and ethanolamine-HCl was bought from Merck (Darmstadt, Germany). Acetate buffer, NT, and BSA was bought from Sigma-Aldrich. Carboxymethyl dextran (CMD) low-density-modified gold surface chips were bought from BioNavis Company (Tampere region, Finland). Other materials utilized were of the highest quality.

2.2. Stock preparation

Phosphate buffer was prepared by dissolving a tablet of saline phosphate buffer in deionized water. The stock solution of BSA (1.4×10^{-5} M, according to its molecular weight of 66,000D) was dissolved in a 0.01 M phosphate buffer solution (pH 7.40). NT stock solution at a concentration of 2 mM was prepared by dissolving 1.4 mg NT in PBS buffer solution. All ready solutions were stored in the refrigerator at 4 °C.

2.3. Fluorescence experiments

Fluorescence spectroscopy evaluations were performed at five distinct temperatures with a Jasco FP-750 fluorescence spectrometer (Jasco International Co, Kyoto, Japan) equipped with a thermostat. The measurements were done in a 10 mm quartz cell. To observe the fluorescence of Trp residues, a wavelength of 290 nm was used for excitation. The slit width for excitation and emission was 5.0 nm. The scanning speed of the device was set to 8000 nm/min. 1 mM BSA solution was titrated with concentrations of $1^{-6} \times 10^{-5}$ and its fluorescence spectrum was recorded at a wavelength of 300–450 nm. All measurements were performed with PBS buffer at 288, 293, 398, 303, and 310 K. To eliminate the inner filter effects of protein and ligands, absorbance measurements were performed at the excitation and emission wavelengths of the fluorescence measurements. The fluorescence intensity was corrected using Eq. (1):

$$F_{\text{cor}} = F_{\text{obs}} 10^{(A_1 + A_2)/2} \quad (1)$$

where F_{cor} and F_{obs} are the fluorescence intensity corrected and observed, respectively, while A_1 and A_2 are the sums of the absorbance of protein and ligand at excitation and emission wavelengths, respectively (Marouzi et al., 2017).

2.4. UV–Vis spectrophotometry

To record Absorption spectra of BSA without and with different concentrations of NT at a temperature of 25 °C, a UV–Vis spectrometer model T70 + manufactured by PG Instrument Company (Leicestershire, UK) was used. Titration of 1 mM BSA solution with distinct concentrations of NT (0–70 μM) was performed in a 10 mm quartz cuvette. Finally, the solution was thoroughly blended and incubated for up to 3 min to let NT interact with BSA.

2.5. SPR measurements

To investigate the interaction of BSA with NT and calculate the kinetic parameters, an SPR device (MP-SPR navi210 A, Bionavis Ltd, Tampere, Finland) with a dual-stream channel (using Kerchman's prism configuration) and a continuous peristaltic pump was used (Sharifi et al., 2017).

2.6. Immobilization of BSA on CMD sensor chip

The CMD sensor chip was settled within the SPR instrument. Acetate buffer (10 mM) with pH 4.5 was utilized to wash the entire machine. After 15 min, the sensor diagram reached the baseline, then NaCl (2 M) and NaOH with concentration (0.1 M) were used to clear the SPR channels for 3 min at a speed of 30 $\mu\text{l}/\text{min}$. In the next step to activate the carboxyl groups on the CMD sensor chip, a stream of solution (NHS 0.05 M + EDC 0.2 M) EDC/NHS in equal ratios of 1:1 was injected into the SPR instrument at a speed of 30 microliters per min for 7 min. Then, to stabilize BSA on the CMD sensor chip, a solution of BSA at a concentration of 1 mg/ml was infused into channel 1 for 7 min and acetate buffer was infused simultaneously into channel 2. Finally, a stream of Ethanolamine-HCl solution (1 M, pH 8.5) was injected at an

amount of 30 $\mu\text{l}/\text{min}$ to inactivate and block the active carboxyl groups on the surface of the CMD chip (Sharifi et al., 2017; Fathi et al., 2019).

2.7. Kinetic parameters analysis of BSA interaction with NT

To calculate the kinetic parameters including association constant (K_a), dissociation constant (K_d), and equilibrium constants (K_D), which are calculated via $K_D = k_d/k_a$, different concentrations of NT were prepared in PBS buffer with pH 7.4 and stream of the prepared solution at a speed of 30 $\mu\text{l}/\text{min}$ for 2 min at 293, 298, 303, and 310 K was injected into both flow cells. Since BSA was immobilized in only one channel, both stream cells were utilized for sample injection and the stream cell without BSA was utilized as a reference. The need for the regeneration process is eliminated due to the rapid separation of NT from the BSA level. By measuring the SPR signal, the amount of binding of NT to BSA was determined. DrawerTM for SPR NaviTM was used to determine the kinetic parameters upon BSA interaction with NT (Maleki et al., 2020).

2.8. Study of molecular docking

To understand the possible interaction of NT with BSA as a potential target biomolecule, a molecular docking study was conducted via the AutoDock 4.2 package, which is validated by The Scripps Research Institute, La Jolla, CA, USA. The 3D molecular building of NT was achieved from the PubChem website (PubChem CID:5284447) (<https://pubchem.ncbi.nlm.nih.gov/>), and following that, its structure was optimized for our calculation through Gaussian 03 software (B3LYP method). Next, the BSA crystal structure (PDB code: 3 V03, 2.7 Å) was downloaded from Protein Data Bank Website (<https://www.rcsb.org/>). AutoDock Tools-1.5.6 program was used to apply Kollman/Gasteiger charges to the BSA structure (subunit A), and also eliminate all water molecules. To find the binding domain on BSA, a blind docking calculation was performed at a lace box of 126 × 126 × 126 Å (spacing parameter of 0.523 Å), and then the lowest binding score was considered for further analysis. To focus on the binding site, another docking study was accomplished at a grid box of 70 × 70 × 70 Å and a spacing parameter of 0.380 Å. The Lamarckian genetic algorithm was applied in all calculation runs. The results were displayed and analyzed via UCSF Chimera software (version 1.14).

3. Results and discussion

3.1. Study of BSA fluorescence quenching

The fluorescence quenching analysis was used for the investigation of NT interaction with BSA. It is a useful procedure for the study of protein interaction with various molecules and the evaluation of structural changes induced in the protein on the molecular level (Wani et al., 2018). Among the different types of molecular interactions, we can mention excited-state reactions, molecular rearrangements, energy transfer, ground-state complex formation, and quenching collisions that lead to quenching (Lakowicz, 2006). In general, the innate

fluorescence of BSA is inferred from Trp, Tyr, and Phe. However, among them, the contribution of tryptophan is a maximum (Wu et al., 2019; Javaheri-Ghezeldizaj et al., 2021). Innate fluorescence of BSA is regularly utilized as a test to find the affinity of BSA to various food additives due to the Trp residues presence on the surface of BSA (Trp 134) and the interior of the hydrophobic pocket (Trp 213).

The fluorescent spectrum of BSA in the lack and existence of NT in the PBS buffer (pH = 7.4) is displayed in Fig. 1 (Javaheri-Ghezeldizaj et al., 2020). BSA has an intense fluorescence emission peak of about 350 nm below the excitation wavelength of 290 nm, and after adding NT from 0 to 60 μM , a decline in fluorescence spectra was recorded without any significant change in the emission wavelength. This trend indicates that the innate fluorescence of BSA is quenching owing to interaction with NT (Javaheri-Ghezeldizaj et al., 2020). Quenching mechanisms can be identified by three factors: temperature, viscosity, and excitation state life. In the static quenching method (by complex formation), increasing the temperature reduces the stability of the base state complex, followed by a reduction of the quenching constant (K_{SV}), and therefore the formation of a ligand-protein complex with non-fluorescent properties (independent of diffusion) (Tantimongcolwat et al., 2019). In dynamic quenching, on the other hand, the absorption spectrum is not affected by extinction because it is effective only in the excitation mode of the quencher (Taheri et al., 2022). In dynamic quenching, high temperature causes quicker dissemination steady and progresses electron transfer, and therefore, K_{SV} tends to increase (Wani

et al., 2018; Banu et al., 2021). The Stern-Volmer steady-state Eq. (2) was utilized to confirm the nature of the BSA fluorescence quenching mechanism due to the formation of the complex with NT (Javaheri-Ghezeldizaj et al., 2020).

$$\frac{F_0}{F} = 1 + K_{SV}[Q] = 1 + k_q\tau_0 \quad (2)$$

According to Eq. (2), F_0 and F show the intensity of BSA fluorescence in the lack and existence of NT (quencher). K_{SV} (Stern-Volmer constant), $[Q]$ indicates the initial concentration of the quencher, k_q is the quenching rate of biomolecules of a protein (BSA) and τ_0 is the lifespan of the exciting mood of the protein in the lack of any quencher (Maheri et al., 2022). K_{SV} values can be attained by the slope of the F_0/F plotting versus $[Q]$. The K_{SV} values are important from the viewpoint of fluorescence quenching. As revealed in Fig. 2A and Table 1, there is a powerful linear connection between F_0/F and $[Q]$ for the Stern-Volmer diagram. Static and dynamic quenching can result in a Stern-Volmer linear diagram. The difference is that in hybrid mechanisms the diagram is nonlinear and this diagram shows an upward curvature. In general, with a raising temperature, the K_{SV} values decrease in the static quenching process but in the dynamic quenching process, temperature rising leads to a constant increase in diffusion and promotes electron transmission, so K_{SV} tends to increase (Shi et al., 2017; Mahmoudpour et al., 2020; Javaheri-Ghezeldizaj et al., 2021). K_{SV} and k_q values are shown in Table 1. Considering the K_{SV} values increase from 288 to 310 K (5.32×10^3 to 10.0×10^3) indicates that fluorescence quenching is more

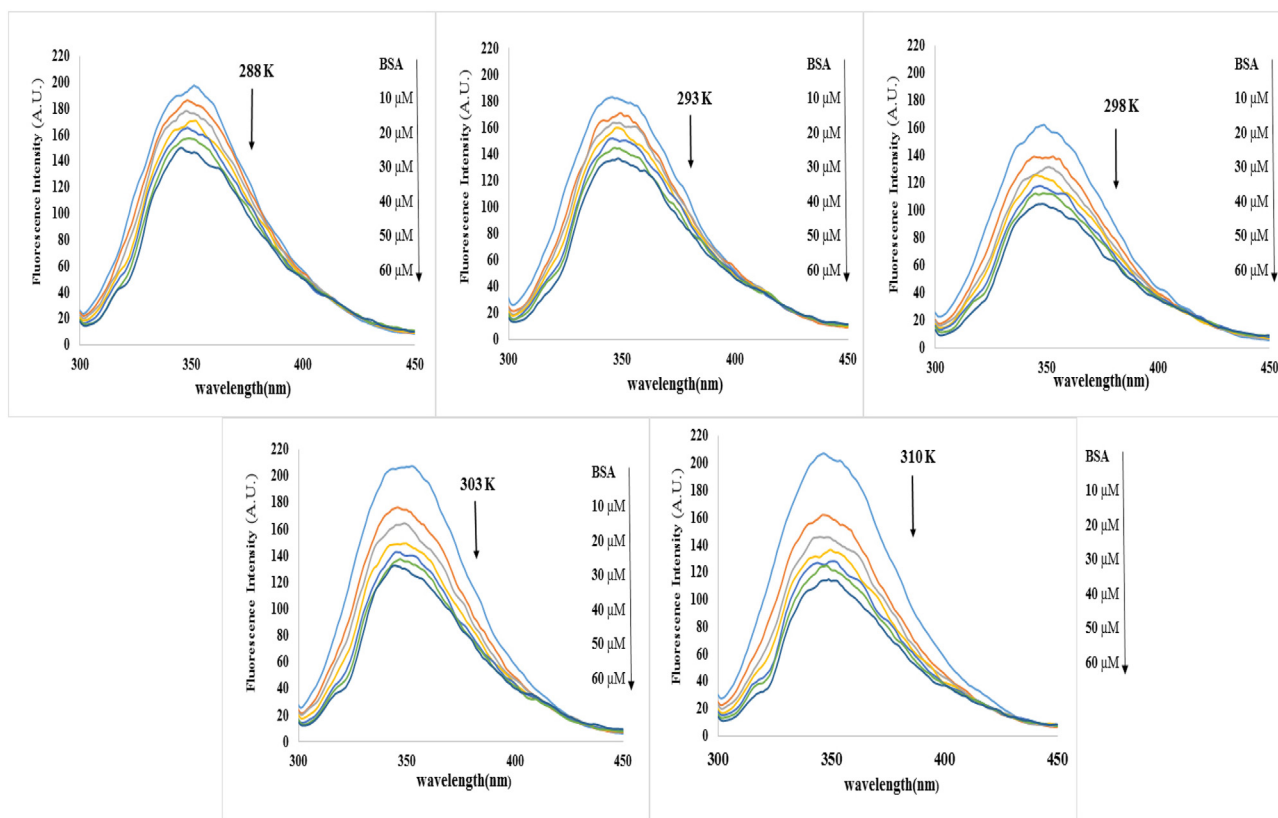


Fig. 1 Inherent fluorescence spectrum of BSA (2 mM) in the absence and presence of various NT concentrations (0, 10, 20, 30, 40, 50 and 60 μM) at 288, 293, 298, 303, and 310 K temperature.

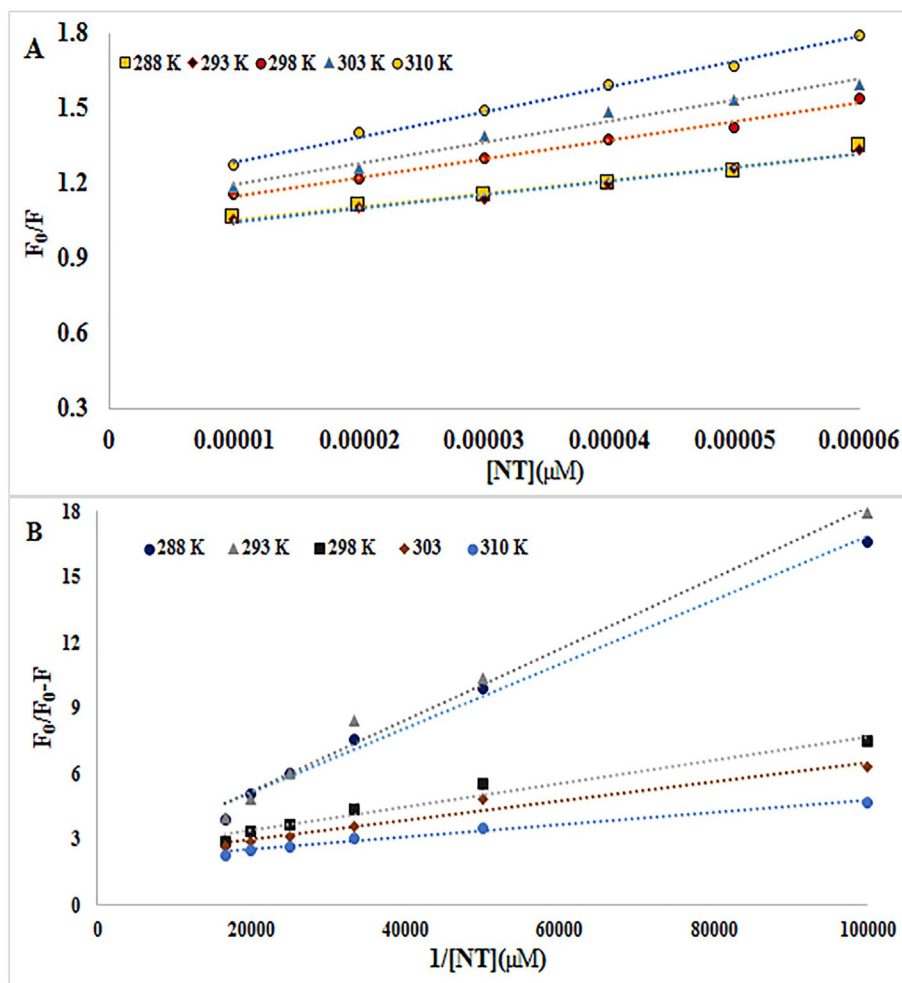


Fig. 2 A) The Stern–Volmer diagrams of the quenching of BSA fluorescence by NT at five different temperatures B) Modified Stern–Volmer plots for quenching of BSA upon interaction with NT at five different temperatures.

Table 1 Stern–Volmer quenching constants (K_{sv}), effective quenching constant for the accessible BSA (k_a), quenching rate constant (k_q), binding constant (K_b) and relative thermodynamic parameters of BSA–NT complex for the interaction between BSA and NT in the five temperatures.

T (K)	K_{SV} ($10^3 M^{-1}$)	K_q ($10^{12} M^{-1}S^{-1}$)	K_a ($10^3 m^{-1}$)	K_b ($10^2 M^{-1}$)	ΔH° (kJ mol $^{-1}$)	ΔS° (J mol $^{-1} K^{-1}$)	ΔG° (kJ mol $^{-1}$)	R^2
288	5.32	0.88	21.696	18.73			−18.73	0.97
293	5.48	0.91	9.650	31.49			−17.54	0.98
298	7.47	1.24	47.334	3.77	−87.16	−237.6	−16.35	0.98
303	8.37	1.39	51.995	4.07			−15.16	0.97
310	10.01	1.66	65.760	2.13			−13.50	0.99

compatible with dynamic quenching instead of static quenching. However, at different temperatures, the k_q values are more than the maximum collision quenching constant ($2.0 \times 10^{10} Lmol^{-1}s^{-1}$), signifying the occurrence of static quenching. Therefore, it can be inferred that NT reduced the fluorescence of BSA via a hybrid quenching mechanism (Sandhya et al., 2011; Shi et al., 2017; Nan et al., 2019; Javaheri-Ghezeldizaj et al., 2021).

Fluorescence quenching data were additionally evaluated by a modified Stern–Volmer Eq. (3) (Ali et al., 2023):

$$\frac{F_0}{\Delta F(F_0 - F)} = \frac{1}{f_a K_a} \times \frac{1}{[Q]} + \frac{1}{f_a} \quad (3)$$

where, f_a and K_a (M^{-1}) denote the fraction of reachable fluorescence and the effective quenching constant for the accessible BSA, respectively. Fig. 2B and Table 1 show modified Stern–Volmer plots for five dissimilar temperatures and relevant results, respectively. The decrease in the K_a value upon rising temperature is demonstrative of quenching fluorescence through the static mechanism while an increasing amount of it

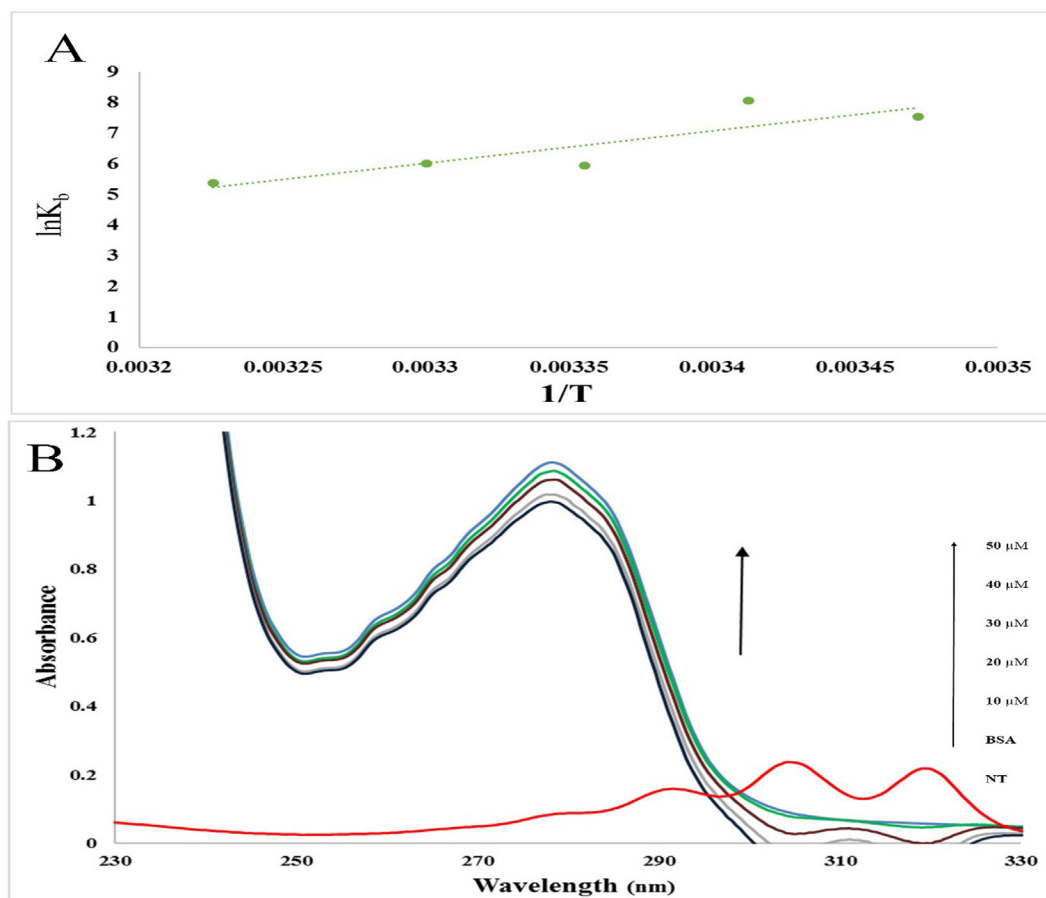


Fig. 3 A) The van't Hoff diagrams for the interaction of BSA with NT B) Absorption spectra of BSA (2 mM) before and after the addition of NT (0, 10, 20, 30, 40, and 50 μM). The red line showed the absorption spectra of NT.

showed the happening of dynamic quenching mechanism. However, the attained values of K_a did not show a regular increasing or decreasing trend upon rising temperature from 288 K to 310 K, which additionally approved the occurrence of BSA fluorescence quenching via a hybrid mechanism (a both static and dynamic quenching mechanism) (Shaghghi et al., 2022).

3.2. Binding constant and number of binding locations

If small molecules such as NT interact separately with a set of equivalent sites on biomacromolecules such as BSA, the possible binding stoichiometry (n) and the binding constant (K_b) of NT-BSA can be analyzed by the slope and intercept double logarithm regression curve utilizing the following equation (Bhojwani et al., 2023):

$$\log \frac{(F_0 - F)}{F} = \log K_b + n \log [Q] \quad (4)$$

where F_0 , F , and $[Q]$ are the same as the Eq. (2) parameters, K_b is the binding constant for the NT-BSA interaction, and the number of binding locations per protein molecule is represented by n . Usually, the affinity of ligand-protein will increase upon the raising of the K_b value. In this study, the fluorescence data were treated using Eq. (3) by the successive approximation method and the K_b values in various temperatures were shown in Table 1. The K_b calculated for BSA-NT systems in-

ferred reasonable binding affinity compared to other strong BSA-ligand complexes with binding constants ranging from 10^3 to 10^5 M^{-1} . The outcomes displayed that the K_b values decrease upon rising temperatures, in other words, it can be deduced that high temperatures can decrease the stability of this complex. Similarly, it can be concluded that in low concentrations of NT, binding is comparably stronger and it becomes closer to the tryptophan residues (Min et al., 2004; Sani et al., 2018). Considering the relatively high binding constant value obtained for NT ($2.13 \times 10^2 \text{ M}^{-1}$) at 310 K (body temperature) and the fact that SA is the most abundant biological molecule in the circulatory system of many living organisms and is also responsible for several physiological functions such as transfer of exogenous and endogenous compounds (fatty acids, drugs, steroids, metal particles, and metabolites), it can be concluded that NT has capability to interact with serum albumin in the bloodstream.

3.3. Analysis of thermodynamic parameters

Intramolecular interaction forces consist of electrostatic bonding, hydrogen bonding, van der Waals forces, and hydrophobic interactions that play a significant function in protein binding to various ligands. Enthalpy change (ΔH°), Gibbs free energy (ΔG°), and entropy change (ΔS°) are among the thermodynamic parameters, which help to identify the type of forces influencing the interaction between two molecules. Pos-

itive values of ΔH° and ΔS° represent the presence of hydrophobic interaction between two molecules and negative values of ΔH° and ΔS° are signs of van der Waals forces or hydrogen bonds occurring. A value of ΔG° less than zero indicates that a spontaneous interaction between NT and BSA occurs at the appropriate temperature. Finally, a negative sign for Δ° indicates that the interaction of NT with BSA is enthalpy-driven. Thermodynamic parameters can be calculated by the following van't Hoff and Gibbs free energy Eqs. (5) and (6):

$$\ln K_b = -\frac{\Delta H^\circ}{RT} + \frac{\Delta S^\circ}{R} \quad (5)$$

$$\Delta G^\circ = \Delta H^\circ - T\Delta S^\circ \quad (6)$$

According to Eq. (5), R is the universal gas constant ($8.314 \text{ J mol}^{-1} \text{ K}^{-1}$) and T describes the experiential temperature. Van't Hoff diagrams for the interaction of BSA and NT

are demonstrated in Fig. 3A. The values for ΔH° , ΔG° , and ΔS° at five temperatures are given in Table 1. The results revealed that the values of ΔS° and ΔH° are $-237.6 \text{ J mol}^{-1} \text{ K}^{-1}$ and $-87.16 \text{ kJ mol}^{-1}$, respectively. Negative values of ΔH° and ΔS° confirmed that van der Waals forces, or hydrogen bonds, are the basic forces in the interaction of NT with BSA (Ross and Subramanian, 1981; Zhang et al., 2012; Wani et al., 2017; Wani et al., 2018; Wu et al., 2019; Javaheri-Ghezeldizaj et al., 2020).

3.4. UV-Vis absorption spectroscopy

UV-Vis spectrum measurement is a procedure for analyzing structural changes and recognizing the formation of protein complexes upon interaction with small molecules, which is used in protein-ligand research. In this study, we evaluated the interaction of BSA with different amounts of NT using

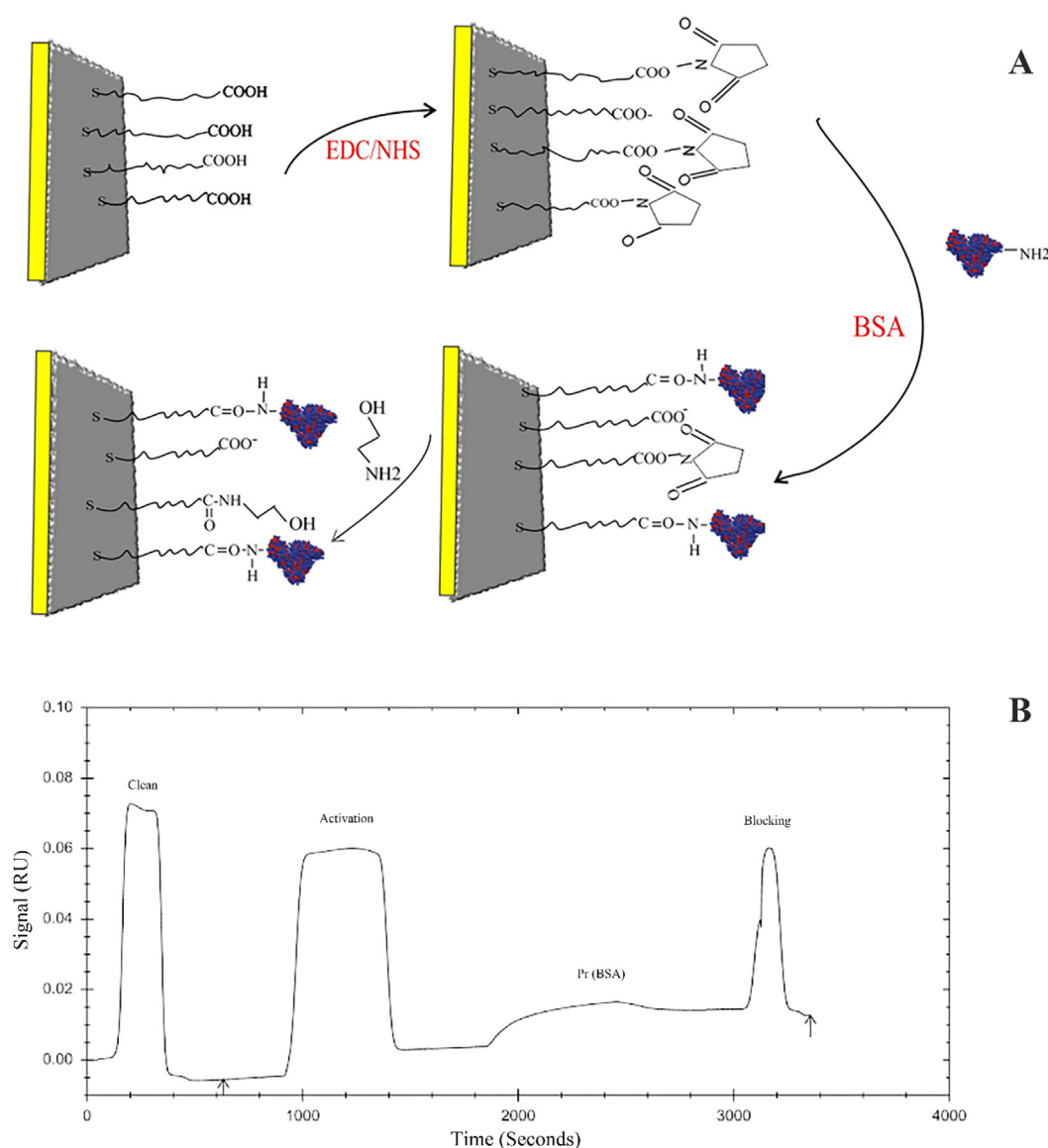


Fig. 4 A) Schematic plot of BSA immobilization by amine coupling. B) SPR sensorgram of BSA immobilization processes on a CMD chip.

UV-Vis spectroscopy. Owing to the presence of aromatic amino acid residues (tryptophan, phenylalanine, and tyrosine residues) in the BSA structure, an innate absorption peak of about 210 (sharp peak) and 280 (weak peak) nm can be seen in Fig. 3B. By adding different amounts of NT (10 to 60 μM) to the BSA solution, the BSA adsorption spectra at 280 nm gradually increased. In general, abnormalities in the albumin absorption spectrum in the formation of the albumin ligand complex are evident. Based on this, it can be concluded that the change in the structure and microenvironment of BSA was owing to the interaction with NT and the formation of the BSA-NT complex (Hu et al., 2006; Banu et al., 2021).

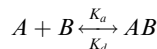
3.5. Immobilization of BSA on CMD sensor chip

A schematic illustration of the BSA immobilization on the surface of a gold chip via amide linkage is shown in Fig. 4A (Fathi et al., 2019). As can be seen in the figure, the carboxylic groups on the surface of the CMD chip were activated using the EDC/NHS solution injected into the device. And in the next step, by injecting BSA into the device, a association was established between the active carboxyl groups on the surface of the CMD chip and BSA, and thus BSA was stabilized on the surface of the chip. In the last step, ethanolamine solution was used to block unreacted sites (Maleki et al., 2020). The sensorgram of these steps is shown in Fig. 4B. Measurements showed that

at pH 7.4 the immobilization level of BSA on the CMD chip surface was acceptable (Taghipour et al., 2018).

3.6. Kinetic parameters of BSA interaction with Natamycin

The reversible reaction of BSA-NT complex formation and separation can be shown by a simple Langmuir reaction:



To calculate the kinetic properties, it is necessary to calculate the k_a , k_d , and K_D for the binding of BSA to NT. The association constant is denoted by k_a , while the dissociation is denoted by k_d .

BSA sensorgrams in the existence and lack of various concentrations of NT (0.1–1.2 μM) at four temperatures (298, 303, 308, and 310 K) have been shown in Fig. 5 and its related data has been demonstrated in Table 2. The k_a of the BSA interaction with NT decreased when temperature increased while the k_d of the interaction was constant and therefore the values of K_D have been increased. The attained results demonstrated that the values of k_a play a major role in the variation of K_D values. Besides, increasing K_D values upon raising temperature indicated that BSA binding to NT decreased, which verified the attained data from the calculation of binding constants through a fluorimetry study.

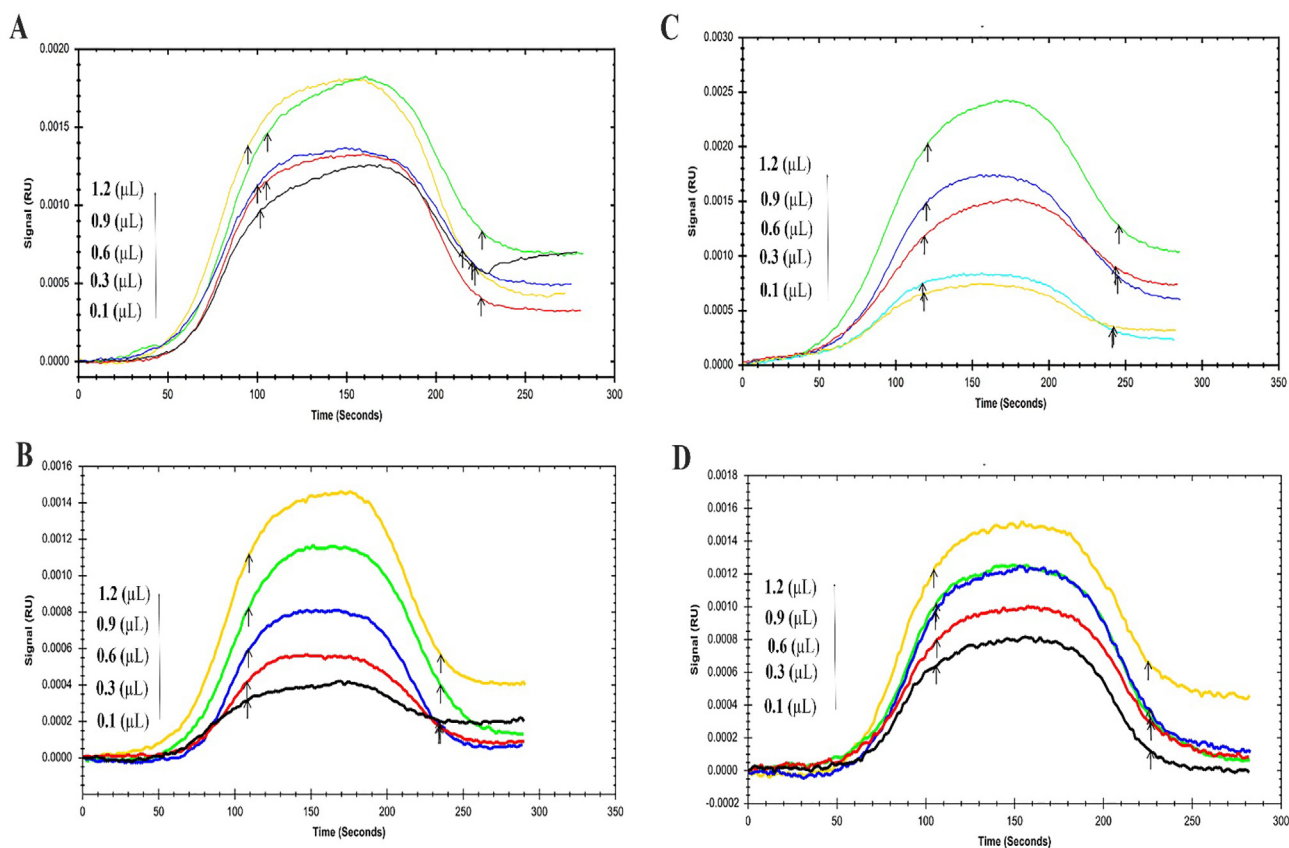


Fig. 5 The SPR Sensorgram of immobilized BSA interaction with various concentrations of NT as a food additive at four temperatures (A) 293 °K, (B) 298 °K, (C) 303 °K, and (D) 310 °K.

Table 2 Association rate (k_a), dissociation rate (k_d), and equilibrium constant (K_D) values of NT interaction with BSA.

T (K)	$k_a(1/M \times s)$	$k_d(1/s)$	$K_D(M)$
293	2.15×10^4	1.00×10^{-3}	4.65×10^{-8}
298	1.04×10^4	1.00×10^{-3}	9.87×10^{-8}
303	1.01×10^4	1.00×10^{-3}	9.94×10^{-8}
310	9.98×10^3	1.00×10^{-3}	1.00×10^{-7}

3.7. Molecular docking results

One of the most widely used methods for studying the interaction of small molecules with biomolecules is the study of molecular binding. In the present study, the interaction of the NT and BSA biomolecule was investigated by applying of Auto Dock 4.2 package. The tertiary structure of BSA is classified into three binding domains (homologous), which are nominated as I, II, and III with subdomains A and B. The major ligand-binding region is located in some hydrophobic pockets in subdomain IIIA (Szymaszek et al., 2022).

In the present study, the blind docking study displayed that NT could bind to a pit that is located among IIIA (Sudlow I) and IB domains (Fig. 6A). Sudlow I is an important binding site on BSA that several big molecules enable to bind there

due to the extended entrance gate. The importance of Sudlow I lies in its ability to bind a wide range of drugs, which makes it a useful element for drug delivery and development. Many drugs, including non-steroidal anti-inflammatory drugs (NSAIDs), antibiotics, and anti-cancer agents, bind to Sudlow I with high affinity, leading to their sequestration in the plasma and reduced toxicity. Moreover, the binding of drugs to the Sudlow I site in BSA alters the pharmacokinetics and pharmacodynamics of the drugs. It affects the duration of drug action, the volume of distribution, the metabolism, and the elimination of the drug (Solanki et al., 2021).

To provide more details, another docking calculation was carried out with a particular focus on Site II. This site is known as an important position for the binding of many heterocyclic and aromatic compounds. Some studies also reported that Site II is an essential position for binding some fatty acids onto serum albumin (Tayeh et al., 2009; Belatik et al., 2012).

As indicated in Fig. 6B, Ser 109, Asp 111, Lys 114, Leu 115, Glu 424, and Arg 458 have an important role in NT-BSA interaction. The sign and magnitude of ΔS° and ΔH° indicated that the main significant interaction force for the binding between NT and BSA was van der Waals forces or hydrogen bond (Cheng, 2012). The binding was predicted to be -36.52 kJ mol $^{-1}$, which confirms the spontaneous binding of this ligand onto BSA without any requirement for external energy. As shown in Table 1, the thermodynamic study found the binding free energy (ΔG°) of the NT-BSA complex to be

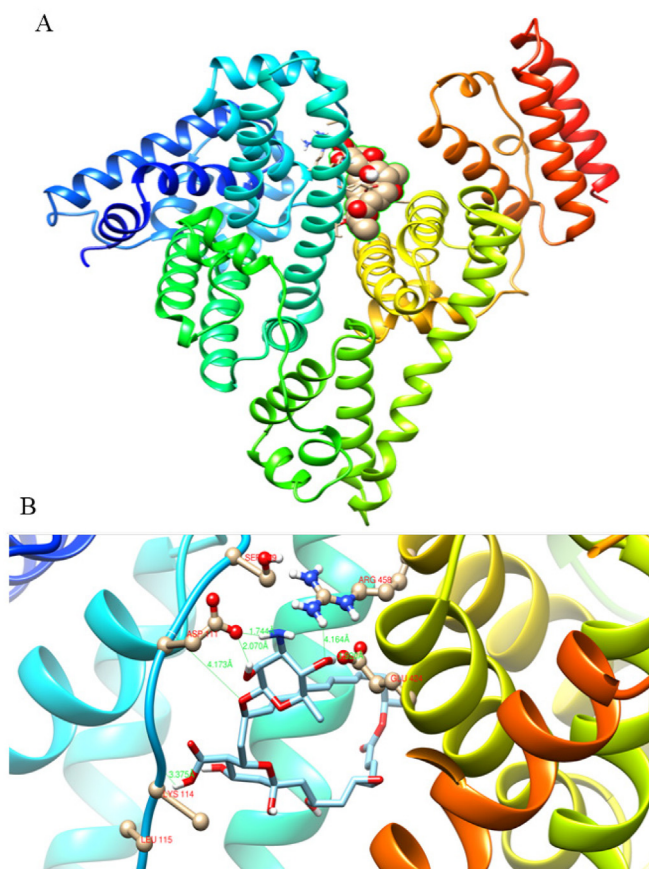


Fig. 6 A) Represents the binding site of NT on BSA in a cavity that is located among IIIA and IB. B) The detailed interaction between NT molecule and BSA on IIA and IB binding domains.

–16.35 kJ mol⁻¹ at room temperature, but this varied from the molecular docking calculation. It is assumed that the theoretical research did not consider interstitial water molecules and buffer salts in the structure of BSA, which could have contributed to the association between NT and BSA molecules via the hydrogen bonding network (Diana et al., 1989; Abou-Zied and Al-Lawatia, 2011).

4. Conclusion

In the current study, the interaction between NT and BSA was explored using different spectroscopic techniques, SPR techniques, and molecular docking modeling. The results of fluorimetry measurements showed that NT reduces the intensity of BSA fluorescence by forming a complex with BSA through a hybrid quenching mechanism. Negative values of both ΔH° and ΔS° confirm that van der Waals forces or hydrogen bonds are the basic forces in the interaction of NT with BSA. The negative ΔG° value confirmed the spontaneous binding of this ligand onto BSA without any requirement for external energy. The results of the blind docking at molecular docking study displayed that NT could bind to a pit that is located among IIIA (Sudlow I) and IB domains. In addition, Ser 109, Asp 111, Lys 114, Leu 115, Glu 424, and Arg 458 also play important roles in NT-BSA interaction.

Declaration of Competing Interest

The authors declare that they have no known competing financial interests or personal relationships that could have appeared to influence the work reported in this paper.

Acknowledgments

The authors would like to thank Tabriz University of Medical Sciences for supporting this project (grant No: 69708), which was a part of my M.Sc thesis.

References

- Abou-Zied, O.K., Al-Lawatia, N., 2011. Exploring the drug-binding site Sudlow I of human serum albumin: the role of water and Trp214 in molecular recognition and ligand binding. *Chem-PhysChem* 12, 270–274. <https://doi.org/10.1002/cphc.201000742>.
- Additives, E. P. o. F., N. S. a. t. Food, 2009. Scientific Opinion on the use of natamycin (E 235) as a food additive. *EFSA J.* 7, 1412.
- Ali, M.S., Rehman, M.T., Al-Lohedan, H.A., et al., 2023. Study of the binding of cuminaldehyde with bovine serum albumin by spectroscopic and molecular modeling methods. *J. Spectroscopy* 2023.
- Assaran Darban, R., Shareghi, B., Asoodeh, A., et al., 2017. Multi-spectroscopic and molecular modeling studies of interaction between two different angiotensin I converting enzyme inhibitory peptides from gluten hydrolysate and human serum albumin. *J. Biomol. Struct. Dyn.* 35, 3648–3662. <https://doi.org/10.1080/07391102.2016.1264892>.
- Banu, A., Khan, R.H., Qashqoosh, M., et al., 2021. Multispectroscopic and computational studies of interaction of bovine serum albumin, human serum albumin and bovine hemoglobin with bisacodyl. *J. Mol. Struct.* 1249, <https://doi.org/10.1016/j.molstruc.2021.131550>.
- Basu, A., Suresh Kumar, G., 2015. Thermodynamics of the interaction of the food additive tartrazine with serum albumins: A microcalorimetric investigation. *Food Chem.* 175, 137–142. <https://doi.org/10.1016/j.foodchem.2014.11.141>.
- Belatik, A., Hotchandani, S., Carpentier, R., et al., 2012. Locating the binding sites of Pb(II) Ion with human and bovine serum albumins. *PLoS One* 7, e36723.
- Bhojwani, H., Begwani, K., Bhor, V., et al., 2023. Synthesis and biological evaluation of benzamide-chalcone hybrids as potential c-Met kinase and COX-2 inhibitors. *Arch. Pharm.* e2200405.
- Brik, H., 1981. Natamycin. *Analytical Profiles of Drug Substances* vol. 10, 513–561.
- Cheng, Z., 2012. Studies on the interaction between scopoletin and two serum albumins by spectroscopic methods. *J. Lumin.* 132, 2719–2729.
- da Silva, M.A., Bierhalz, A.C.K., Kieckbusch, T.G., 2012. Modelling natamycin release from alginate/chitosan active films. *Int. J. Food Sci. Technol.* 47, 740–746.
- Dalhoff, A.A., Levy, S.B., 2015. Does use of the polyene natamycin as a food preservative jeopardise the clinical efficacy of amphotericin B? A word of concern. *Int. J. Antimicrob. Agents* 45, 564–567.
- Diana, F.J., Veronich, K., Kapoor, A.L., 1989. Binding of non-steroidal anti-inflammatory agents and their effect on binding of racemic warfarin and its enantiomers to human serum albumin. *J. Pharm. Sci.* 78, 195–199. <https://doi.org/10.1002/jps.2600780304>.
- Elsayed, E.A., Farid, M.A.F., El Enshasy, H.A., 2013. Improvement in natamycin production by *Streptomyces natalensis* with the addition of short-chain carboxylic acids. *Process Biochem.* 48, 1831–1838.
- Fathi, F., Sharifi, M., Jafari, A., et al., 2019. Kinetic and thermodynamic insights into interaction of albumin with piperacillin: Spectroscopic and molecular modeling approaches. *J. Mol. Liq.* 296, 111770.
- Hu, Y.-J., Liu, Y., Zhao, R.-M., et al., 2006. Spectroscopic studies on the interaction between methylene blue and bovine serum albumin. *J. Photochem. Photobiol. A Chem.* 179, 324–329.
- Inetianbor, J., Yakubu, J., Stephen, E., 2015. Effects of food additives and preservatives on man-a review. *Asian J. Sci. Technol.* 6, 18.
- Javaheri-Ghezeldizaj, F., Mahmoudpour, M., Yekta, R., et al., 2020a. Albumin binding study to sodium lactate food additive using spectroscopic and molecular docking approaches. *J. Mol. Liq.* 310, 113259.
- Javaheri-Ghezeldizaj, F., Soleymani, J., Kashanian, S., et al., 2020b. Multi-spectroscopic, thermodynamic and molecular docking insights into interaction of bovine serum albumin with calcium lactate. *Microchem. J.* 154, 104580.
- Javaheri-Ghezeldizaj, F., Jafari, A., Mahmoudpour, M., et al., 2021. Binding process evaluation of bovine serum albumin and *Lawsonia inermis* (henna) through spectroscopic and molecular docking approaches. *J. Mol. Liq.* 331, 115792.
- Khashkhashi-Moghadam, S., Ezazi-Toroghi, S., Kamkar-Vatanparast, M., et al., 2022. Novel perspective into the interaction behavior study of the cyanidin with human serum albumin-holo transferrin complex: Spectroscopic, calorimetric and molecular modeling approaches. *J. Mol. Liq.* 356, <https://doi.org/10.1016/j.molliq.2022.119042>.
- Koch-Weser, J., Sellers, E.M., 1976. Binding of drugs to serum albumin. *N. Engl. J. Med.* 294, 311–316. <https://doi.org/10.1056/nejm197602052940605>.
- Lakowicz, J.R., 2006. Plasmonics in biology and plasmon-controlled fluorescence. *Plasmonics* 1, 5–33.
- Levy, A., 2007. Does use of the polyene natamycin as a food. *Adv. Drug Deliv. Rev.* 59, 645–666.
- Li, J.-C., Li, N., Wu, Q.-H., et al., 2007. Study on the interaction between clozapine and bovine serum albumin. *J. Mol. Struct.* 833, 184–188.
- Maheri, H., Hashemzadeh, F., Shakibapour, N., et al., 2022. Glucokinase activity enhancement by cellulose nanocrystals isolated from jujube seed: A novel perspective for type II diabetes mellitus treatment (In vitro). *J. Mol. Struct.* 1269, <https://doi.org/10.1016/j.molstruc.2022.133803>.
- Mahmoudpour, M., Javaheri-Ghezeldizaj, F., Yekta, R., et al., 2020. Thermodynamic analysis of albumin interaction with monosodium glutamate food additive: Insights from multi-spectroscopic and molecular docking approaches. *J. Mol. Struct.* 1221, 128785.

- Maleki, S., Dehghan, G., Sadeghi, L., et al, 2020. Surface plasmon resonance, fluorescence, and molecular docking studies of bovine serum albumin interactions with natural coumarin diversin. *Spectrochim. Acta A Mol. Biomol. Spectrosc.* 230, 118063.
- Marouzi, S., Sharifi Rad, A., Beigoli, S., et al, 2017. Study on effect of lomefloxacin on human holo-transferrin in the presence of essential and nonessential amino acids: Spectroscopic and molecular modeling approaches. *Int. J. Biol. Macromol.* 97, 688–699. <https://doi.org/10.1016/j.ijbiomac.2017.01.047>.
- Martínez, M.A., Martínez-Larrañaga, M.R., Castellano, V., et al, 2013. Effect of natamycin on cytochrome P450 enzymes in rats. *Food Chem. Toxicol.* 62, 281–284.
- Min, J., Meng-Xia, X., Dong, Z., et al, 2004. Spectroscopic studies on the interaction of cinnamic acid and its hydroxyl derivatives with human serum albumin. *J. Mol. Struct.* 692, 71–80.
- Mohammadzadeh-Aghdash, H., Dolatabadi, J.E.N., Dehghan, P., et al, 2017. Multi-spectroscopic and molecular modeling studies of bovine serum albumin interaction with sodium acetate food additive. *Food Chem.* 228, 265–269.
- Nan, Z., Hao, C., Ye, X., et al, 2019. Interaction of graphene oxide with bovine serum albumin: A fluorescence quenching study. *Spectrochim. Acta A Mol. Biomol. Spectrosc.* 210, 348–354. <https://doi.org/10.1016/j.saa.2018.11.028>.
- Petitpas, I., Grüne, T., Bhattacharya, A.A., et al, 2001. Crystal structures of human serum albumin complexed with monounsaturated and polyunsaturated fatty acids. *J Mol Biol.* 314, 955–960. <https://doi.org/10.1006/jmbi.2000.5208>.
- Pintado, C.M., Ferreira, M.A., Sousa, I., 2010. Control of pathogenic and spoilage microorganisms from cheese surface by whey protein films containing malic acid, nisin and natamycin. *Food Control* 21, 240–246.
- Rajendiran, N., Thulasidhasan, J., 2016. Spectroscopic, electrochemical and molecular docking studies of dothiepin and doxepin with bovine serum albumin and DNA base. *Luminescence* 31, 1438–1447. <https://doi.org/10.1002/bio.3126>.
- Ross, P.D., Subramanian, S., 1981. Thermodynamics of protein association reactions: forces contributing to stability. *Biochemistry* 20, 3096–3102.
- Sandhya, B., Hegde, A.H., Kalanur, S.S., et al, 2011. Interaction of triprolidine hydrochloride with serum albumins: Thermodynamic and binding characteristics, and influence of site probes. *J. Pharm. Biomed. Anal.* 54, 1180–1186. <https://doi.org/10.1016/j.jpba.2010.12.012>.
- Sani, F.D., Shakibapour, N., Beigoli, S., et al, 2018. Changes in binding affinity between ofloxacin and calf thymus DNA in the presence of histone H1: Spectroscopic and molecular modeling investigations. *J. Lumin.* 203, 599–608.
- Shaghghi, M., Dehghan, G., Rashtbari, S., et al, 2022. Molecular interactions of danofloxacin with bovine serum albumin: An experimental and theoretical investigation. *Iranian J. Anal. Chem.*
- Shahabadi, N., Maghsudi, M., Kiani, Z., et al, 2011. Multispectroscopic studies on the interaction of 2-tert-butylhydroquinone (TBHQ), a food additive, with bovine serum albumin. *Food Chem.* 124, 1063–1068. <https://doi.org/10.1016/j.foodchem.2010.07.079>.
- Sharifi, M., Dolatabadi, J.E.N., Fathi, F., et al, 2017. Kinetic and thermodynamic study of bovine serum albumin interaction with rifampicin using surface plasmon resonance and molecular docking methods. *J. Biomed. Opt.* 22, 037002.
- Shi, J.-H., Pan, D.-Q., Jiang, M., et al, 2017a. In vitro study on binding interaction of quinapril with bovine serum albumin (BSA) using multi-spectroscopic and molecular docking methods. *J. Biomol. Struct. Dyn.* 35, 2211–2223.
- Shi, J.-H., Wang, Q., Pan, D.-Q., et al, 2017b. Characterization of interactions of simvastatin, pravastatin, fluvastatin, and pitavastatin with bovine serum albumin: multiple spectroscopic and molecular docking. *J. Biomol. Struct. Dyn.* 35, 1529–1546.
- Shim, S.-M., Seo, S.H., Lee, Y., et al, 2011. Consumers' knowledge and safety perceptions of food additives: Evaluation on the effectiveness of transmitting information on preservatives. *Food Control* 22, 1054–1060.
- Silva, M.M., Lidon, F., 2016. Food preservatives—An overview on applications and side effects. *Emirates J. Food Agric.*, 366–373.
- Solanki, R., Rostamabadi, H., Patel, S., et al, 2021. Anticancer nano-delivery systems based on bovine serum albumin nanoparticles: A critical review. *Int J Biol Macromol.* 193, 528–540. <https://doi.org/10.1016/j.ijbiomac.2021.10.040>.
- Stark, J., 1999. PRESERVATIVES| Permitted Preservatives—Natamycin.
- Szkudlarek, A., Pożycka, J., Maciążek-Jurczyk, M., 2019. Influence of piracetam on gliclazide—glycated human serum albumin interaction. A spectrofluorometric study. *Molecules.* 24, 111.
- Szymaszek, P., Fiedor, P., Chachaj-Brekiesz, A., et al, 2022. Molecular interactions of bovine serum albumin (BSA) with pyridine derivatives as candidates for non-covalent protein probes: spectroscopic investigation. *J. Mol. Liq.* 347,. <https://doi.org/10.1016/j.molliq.2021.118262> 118262.
- Taghipour, P., Zakariazadeh, M., Sharifi, M., et al, 2018. Bovine serum albumin binding study to erlotinib using surface plasmon resonance and molecular docking methods. *J. Photochem. Photobiol. B Biol.* 183, 11–15.
- Taheri, R., Hamzkanlu, N., Rezvani, Y., et al, 2022. Exploring the HSA/DNA/lung cancer cells binding behavior of p-Syneprine, a naturally occurring phenyl ethanol amine with anti-adipogenic activity: multi spectroscopic, molecular dynamic and cellular approaches. *J. Mol. Liq.* 368,. <https://doi.org/10.1016/j.molliq.2022.120826> 120826.
- Tantimongcolwat, T., Prachayasittikul, S., Prachayasittikul, V., 2019. Unravelling the interaction mechanism between clioquinol and bovine serum albumin by multi-spectroscopic and molecular docking approaches. *Spectrochim. Acta A Mol. Biomol. Spectrosc.* 216, 25–34. <https://doi.org/10.1016/j.saa.2019.03.004>.
- Tayeh, N., Rungassamy, T., Albani, J.R., 2009. Fluorescence spectral resolution of tryptophan residues in bovine and human serum albumins. *J. Pharm. Biomed. Anal.* 50, 107–116. <https://doi.org/10.1016/j.jpba.2009.03.015>.
- Wani, T.A., AlRabiah, H., Bakheit, A.H., et al, 2017. Study of binding interaction of rivaroxaban with bovine serum albumin using multi-spectroscopic and molecular docking approach. *Chem. Cent. J.* 11, 1–9.
- Wani, T.A., Bakheit, A.H., Ansari, M.N., et al, 2018. Spectroscopic and molecular modeling studies of binding interaction between bovine serum albumin and roflumilast. *Drug Des. Devel. Ther.* 12, 2627.
- Wu, J., Bi, S.-Y., Sun, X.-Y., et al, 2019. Study on the interaction of fisetholz with BSA/HSA by multi-spectroscopic, cyclic voltammetric, and molecular docking technique. *J. Biomol. Struct. Dyn.* 37, 3496–3505.
- Xu, H., Yao, N., Xu, H., et al, 2013. Characterization of the interaction between eupatorin and bovine serum albumin by spectroscopic and molecular modeling methods. *Int. J. Mol. Sci.* 14, 14185–14203.
- Zaheri, M., Azimirad, M., Yekta, R., et al, 2023. Kinetic and thermodynamic aspects on the interaction of serum albumin with sodium hydrosulfite: Spectroscopic and molecular docking methods. *J. Photochem. Photobiol. A Chem.* 442,. <https://doi.org/10.1016/j.jphotochem.2023.114804> 114804.
- Zhang, G., Ma, Y., Wang, L., et al, 2012. Multispectroscopic studies on the interaction of maltol, a food additive, with bovine serum albumin. *Food Chem.* 133, 264–270.
- Zunzain, P.A., Ghuman, J., McDonagh, A.F., et al, 2008. Crystallographic analysis of human serum albumin complexed with 4Z, 15E-bilirubin-IX α . *J. Mol. Biol.* 381, 394–406.